

# Sodium-ion Battery Testing

Rachel Carter, Gordon Waller, and Corey Love

Alternative Energy Section

US Naval Research Laboratory

## I. Motivation

Sodium-ion batteries (SIBs) have emerged on the global market and are poised to complement the ubiquitous li-ion battery (LIB). SIBs deliver a lower energy density than LIBs but utilize more globally abundant materials and boasts a higher degree of safety. The cell safety comes from less reactive cathode materials, lower cell energy density, and, in some cases, less flammable electrolytes.<sup>1, 2</sup>

SIBs function much like the LIBs but with larger alkali ions. The larger alkali ion prevents the use of conventional graphite anodes, commonly replaced with hard carbon. Other material compatibility differences result in a wide range of active and passive materials present in SIBs. The wide range of material components make safety risk assessment difficult. Herein we utilize accelerating rate calorimetry<sup>3</sup> and electrochemical analysis to characterize cell safety under storage and transport conditions. This analysis will compare the properties between sodium and lithium batteries.

## II. Methods

A market analysis was completed across SIB manufacturers (Table 1). Multiple parameters, including cell components, form factors, countries of origin and energy densities, were identified as potential metrics for comparison. Three separate SIB manufacturers were evaluated and considered for the project. Of the three SIB manufacturers, cells were acquired from two of them, Company A and Company B.

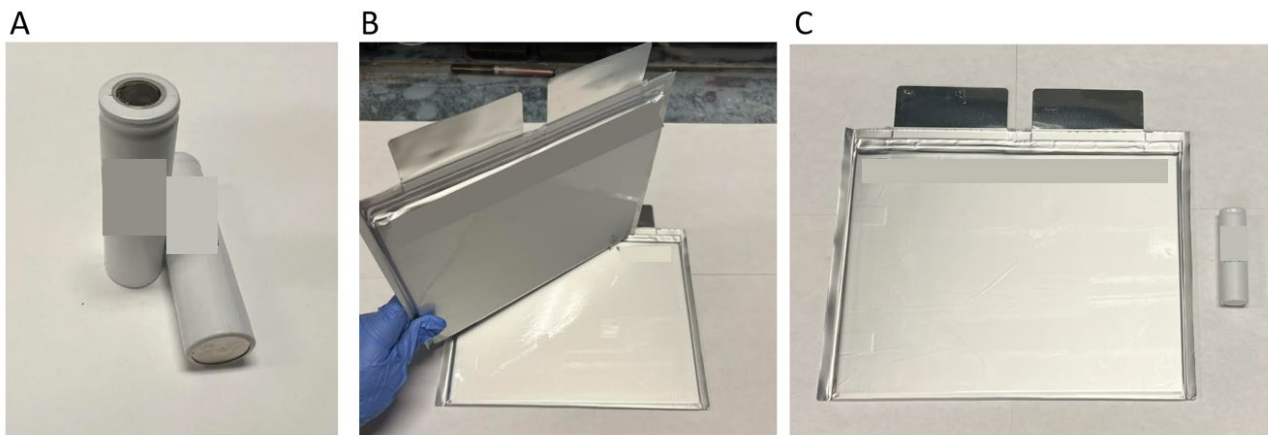


**Figure 1-** Photos of NIB cells. **A** Company A, **B** Company B, and **C** Company A and B.

**Table 1-** Market Research of SIBs physical and electrochemical properties. Italics indicate li-ion battery for reference. Bold indicates cells evaluated in this report. Grey indicates cells not yet available for purchase.

Company (Origin)	Nominal Voltage (V)	Nominal Energy Density (Wh/kg)	Cathode Material	Unit Cell Size (g); Form factor	Other Notes
<i>Samsung Li-ion (Korea)</i>	<i>3.7</i>	<i>263</i>	<i>NMC NiMnCoO</i>	<i>48 18650</i>	<i>High energy</i>
<i>A123 Li-ion (MA, USA)</i>	<i>3.2</i>	<i>110</i>	<i>LFP FePO<sub>4</sub></i>	<i>39 18650</i>	<i>High safety; high power</i>
<b>Company A</b>	<b>3.6</b>	<b>80</b>	<b>NVP Phosphate Na<sub>3</sub>VO<sub>x</sub>(PO<sub>4</sub>)<sub>2</sub>F<sub>y</sub></b>	<b>33 18650</b>	<b>High safety; high power; 30 cells at NRL</b>
<b>Company B</b>	<b>1.8</b>	<b>22</b>	<b>Prussian Blue Na<sub>2</sub>Fe[Fe(CN)<sub>6</sub>]</b>	<b>305 Pouch</b>	<b>High safety/low energy; aqueous; 20 cells at NRL</b>
Company C	3.1	150	Layered metal oxide NaNi <sub>1-x-y-z</sub> M <sup>1</sup> <sub>x</sub> M <sup>2</sup> <sub>y</sub> M <sup>3</sup> <sub>z</sub> O <sub>2</sub>	660 Pouch	Shipped shorted; competitive with LFP; planned in FY23
Company D	3.2	160	Prussian White (R-Na1.92Fe[Fe(CN) <sub>6</sub> ])	Prismatic and Large Cylindrical	FAR Regulated
Company F	3.2	145	Prussian White	Pouch, 26650, 32138	FAR Regulated
Company G	3.2	~100	Prussian White (R-Na1.92Fe[Fe(CN) <sub>6</sub> ])	cylindrical	No battery product yet; selling cathode powders
Company H	2.6	~100	High temperature chemistry (SS) NiCl <sub>2</sub>	Pouch	No product yet; Solid state

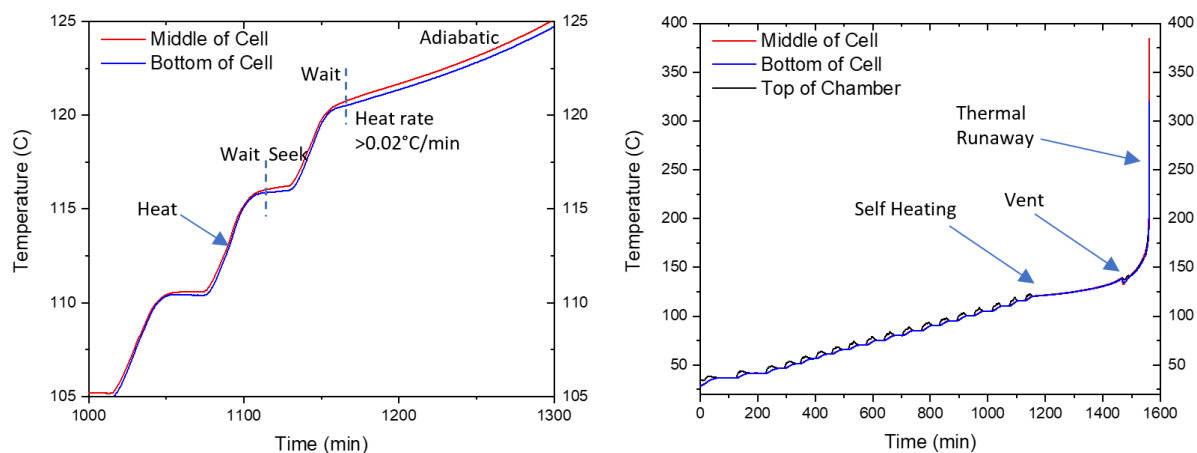


**Figure 2-** Heat-Wait-Seek experiment in ARC EV on 18650 NMC Li-ion cell with key features including vent and thermal runaway indicated.<sup>4</sup>

To assess safety in transport, accelerating rate calorimetry (ARC) was used to characterize thermal stability behavior. This measurement allows calculation of peak heat rates (W and °C/min), peak temperature, and chemical energy of the system (heat of reaction). In contrast, thermal ramp, or isoperiodic assessments only allow peak temperature and the results are dependent on testing setup. In this work, a measurement termed heat-wait-seek (HWS) uses a calorimeter, ARC-EV and ARC-ES manufactured thermal hazard technology and SIB incremented with a thermocouple. The process is visualized in Figure 2. The ambient temperature (25 °C at testing onset) is “heated” in 5 °C increments, the chamber “waits” for equilibrium (40 min) and “seeks” for self-heating or heating of the test article any rate beyond a threshold of 0.2 °C/min. If self-heating is not detected the calorimeter continues to the next 5 °C increment.<sup>3</sup> When self-heating is detected, the chamber approximates adiabatic conditions by maintaining the temperature chamber as close to the self-heating rate of the cell as possible. For battery thermal runaway this test is effective and adiabatic except in the regions where cell-venting and peak heat rates are observed. A cell is considered to be in thermal runaway when the heat rate surpasses 5 °C/min. Li-ion cells like the one shown in Figure 2 often surpass 1000 °C/min.<sup>3</sup> The Company B cell, pouch format was tested in both a “fixtured” and “unfixtured” way. The fixtured method most replicates a single cell with adjacent Company B cells. The fixtured Company B test in the ARC EV are shown in Figure 3.

Electrochemical assessment of cell capacity, rate capability and 0 V tolerance were assessed using MACCOR series 4200 and series 4000 cyclers. Environmental chambers were used to assess various ambient environments.

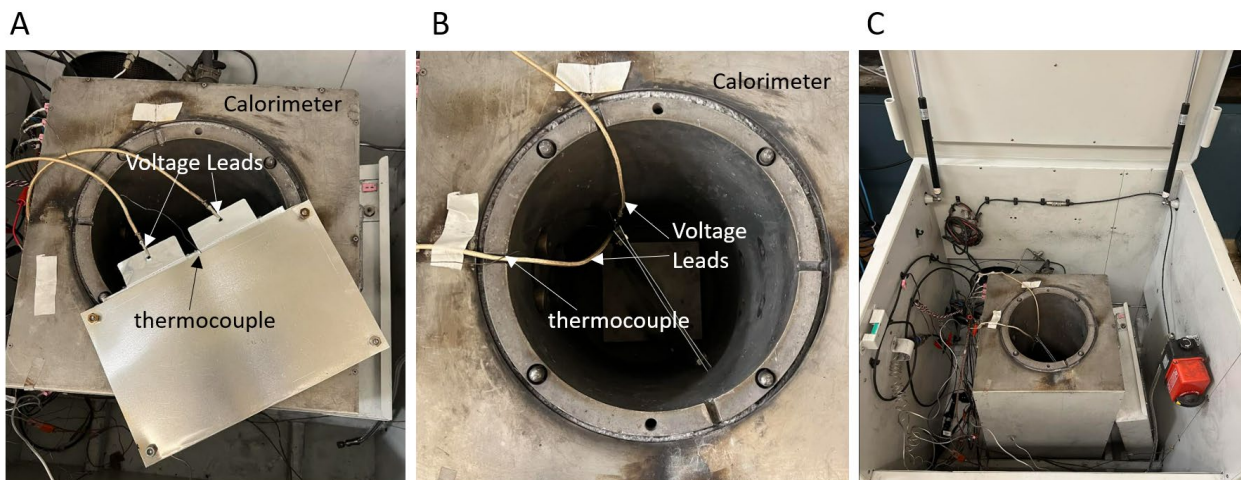


**Figure 3-** **A** Company B cell in aluminum fixture, **B** Cell assembled in ARC EV calorimeter, and **C** Full view of ARC EV.

### III. Accelerating Rate Calorimetry

#### a. Company A

Company A cells were assessed in both the ARC ES and ARC EV. The ARC ES has a smaller enclosure than the ARC EV, providing less excess thermal mass to heat and therefore less overshoot, but the ARC EV provides extensive space for off gassing and unincumbered failure modes. Heat-wait-see tests from each enclosure are shown in Figure 4 A and B, respectively. Cell voltage was collected for the ARC EV test but could not be recorded in the ARC ES test, due to heat loss through the voltage leads. In both tests self-heating onsets at low ambient temperatures,  $\sim 50^\circ$  and  $75^\circ$  C for the ES and EV tests, respectively. These low onset temperatures are initially concerning, since they are below  $100^\circ$  C. However, the heat rates in both remain low ( $< 0.2^\circ\text{C}/\text{min}$  and  $0.2\text{ W}$ ) for both tests (Figure 4 C and D). This heat would easily dissipate to neighboring cells or packaging. Further thermal runaway is not observed in either test. After the onset of self-heating, a vent is observed between  $110$ - $120^\circ$  C. This temperature is similar to the onset of self-heating observed in conventional Li-ion cells, likely due to similar volatile solvents used for the battery electrolyte.<sup>1,3</sup> These solvents are vented off by a pressure release. After the vent, low self-heating ( $< 0.2^\circ\text{C}/\text{min}$  and  $0.1\text{ W}$ ) is observed until the components are burned and the samples are cooled down at a safety temperature of  $300^\circ$  C. The similarity in heat rate from both ARC measurements reveals either calorimeter size is appropriate for safety assessment of this cell.

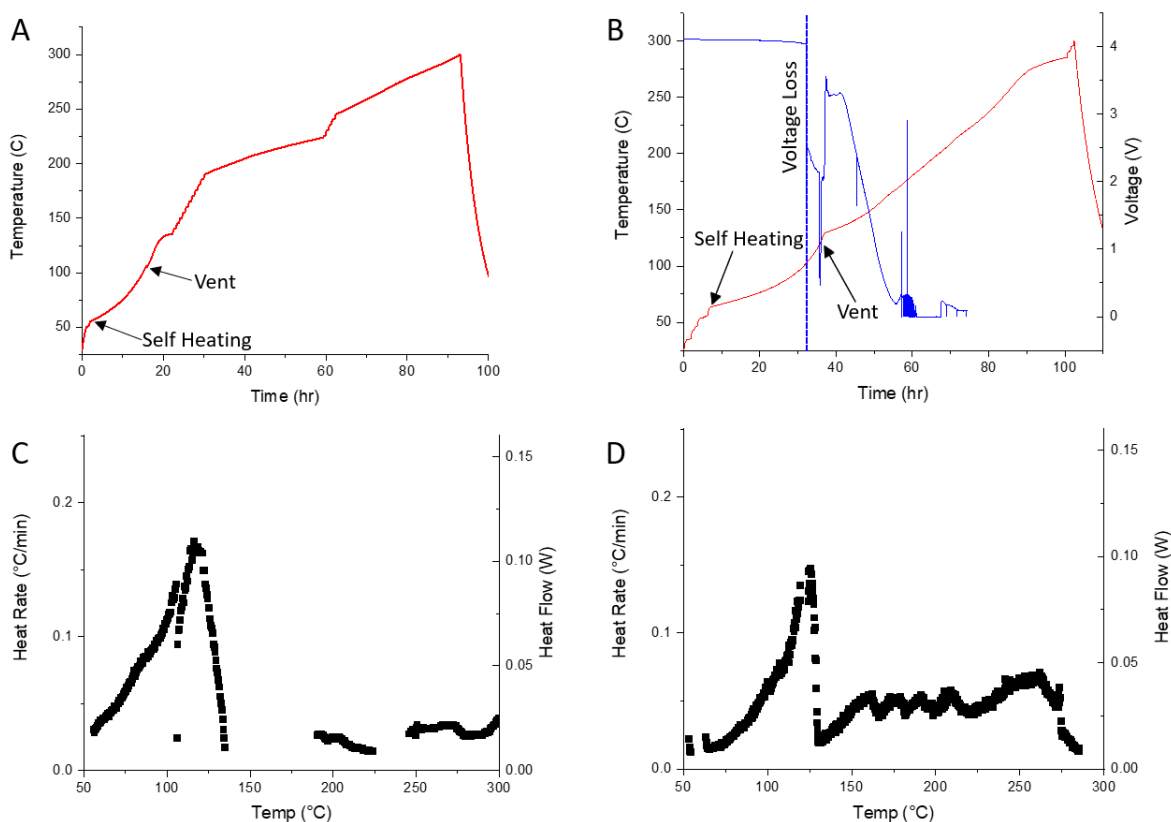


**Figure 4-** HWS experiments of 100% SOC Company A cells in ARC ES **A** and ARC EV **B**. Onset of cell self-heating labeled and location of cell venting. In the ARC EV (**B**), cell voltage was monitored. Heat rate and heat flow with for the ARC ES and ARC EV in **C** and **D** respectively.

To explore the influence of more cells present at the time of failure, 3 cells touching were assessed with the same heat-wait-see test. The energy released from one cell was assessed in Figure 5. This configuration represents larger total electrochemical energy, to determine if this changes the failure mode. In this configuration, self-heating is again onset at about 55 °C. Venting is observed at ~100 °C and self-heating terminates at ~210 °C. The heat rate does not exceed 0.2 °C or 0.12 W. Noting that the threshold for thermal runaway is 5 °C/min. This cell does not experience thermal runaway. After the full test the cell cans maintain their shape and some evidence of material venting through the cap can be seen.

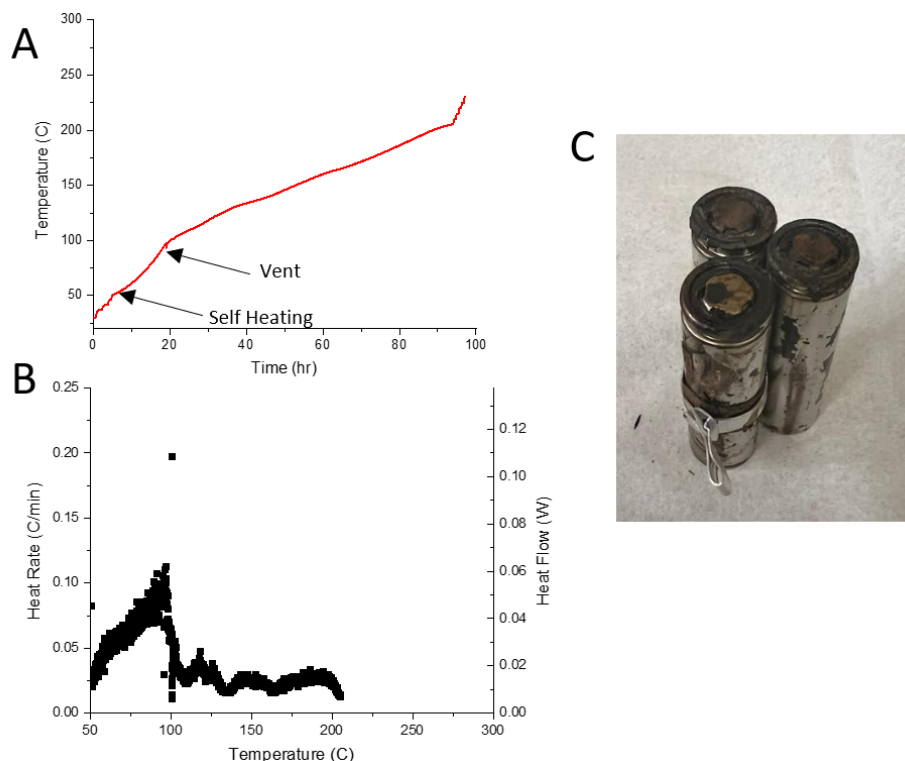


**Figure 5-** **A.** HWS experiments of three 100% SOC Company A cells in a triangle configuration in the ARC ES. Onset of cell self-heating and cell venting on the probed cell. **B** Heat rate and heat flow on the probed cell **C** photograph of the 3 cells after test.

### b. Company B

The Company B cells, which are a large pouch form factor were all tested in the ARC EV due to their size. Here 2 tests were also performed, an “unfixtured” and “fixtured” test. The cells were received at NRL in individual packaging. However, will most commonly be transported in a rack assembly with multiple pouches wired in series and parallel for high current and voltage. Therefore, we wanted to assess the safety implications of each case. The unfixtured case (Figure 6A) exhibited voltage loss and venting at  $\sim 90^{\circ}\text{C}$ . This battery has an aqueous based electrolyte. Therefore, the suppressed voltage loss and venting align with boiling of water. Beyond this point mild self-heating ( $< 1.2^{\circ}\text{C}/\text{min}$  and  $14\text{W}$ ) was observed (Figure 6C). The self-heating rates are higher on this cell compared to the Company A cell because of the higher electrochemical energy (Table 1:  $4.3\text{Ah}$  compared to  $0.7\text{Ah}$ ). Accelerated self-heating is observed at  $200^{\circ}\text{C}$ . However, no catastrophic event is observed via high temperature borescope optical investigation. During self-heating the heat rates remain low ( $< 20\text{W}$ ) and can be dissipated into surrounding environment (packaging, neighboring cells, etc.)

The fixtured Company B cell (Figure 6B) experiences voltage loss and venting at about the same temperature as the unfixtured cell, however self-heating is not detected until  $\sim 175^{\circ}\text{C}$ . This is a demonstration of heat rejected into the cell fixture, reducing self-

heating. We designed a cell fixture of approximately the same mass as the Company B cell, ~290g (Figure 3). This mimics a neighboring cell in a pack. The aluminum plates are shown in Figure 2A, sandwiching the Company B cell. Minimal self-heating was observed ( $<2$  W) in the fixtured cell up to the safety temperature of 300°C.

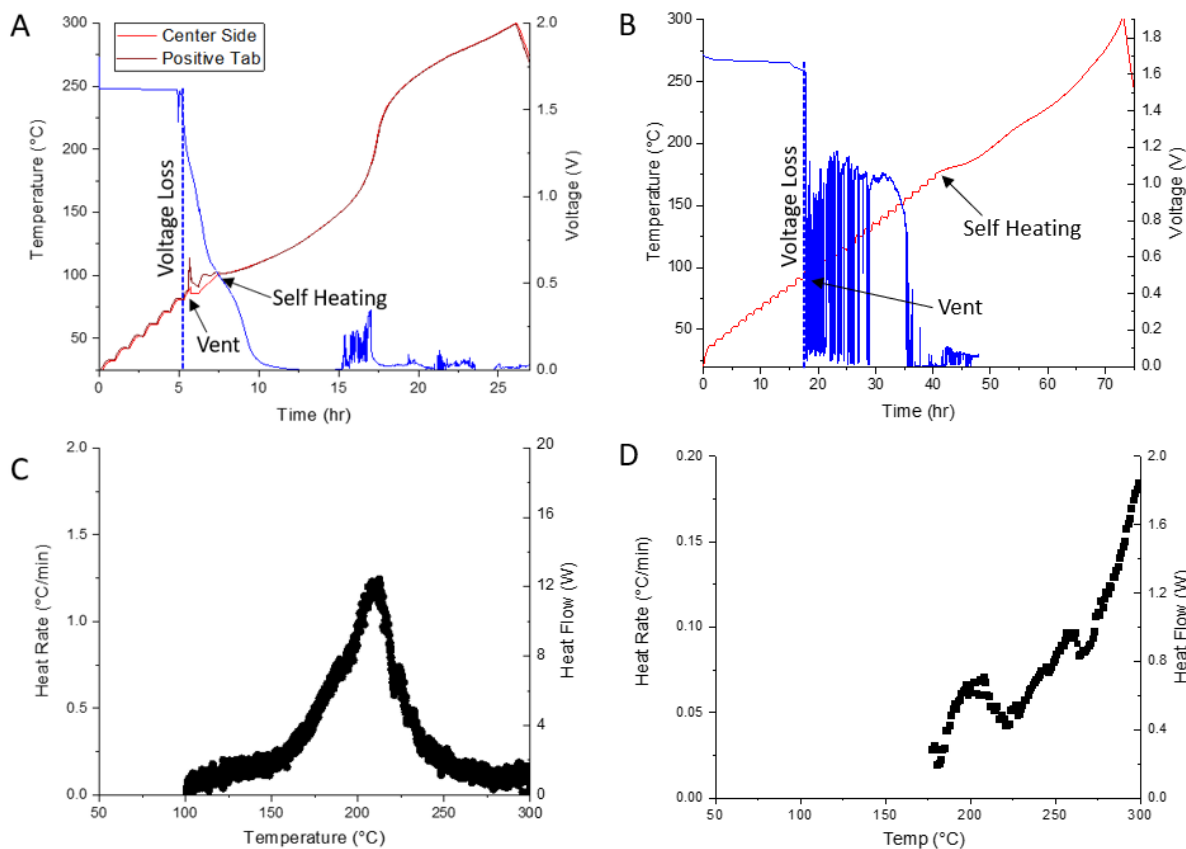


**Figure 6-** HWS experiments of 100% SOC Company B cells in ARC EV unfixtured **A** and fixtured **B**. Onset of cell self-heating labeled, the location of cell venting, and voltage loss. Heat rate and heat flow with for the unfixtured and fixtured cells in **C** and **D** respectively.

In the fixtured configuration, we went on to test 3 cells in a stack in the same fixture (Figure 7). This allowed a higher total energy of Company B cells. The three cells in a stack behave similar to the single cell with loss of voltage and venting observed at about 100 °C but self-heating not observed until about 160 °C. Self-heating is observed until the 300 °C safety temperature. During the self-heating regime, the heat rate does not exceed 0.25 °C/min or 2.5W of heat (Figure 7B). It should be noted that the process of burning the Company B cell resulted on expansion of the cells and damage to the fixture (Figure 7C). Material combustion is expected

to release energy. The key finding is that this behavior is slow and not onset at mild temperatures ( $<100\text{ }^{\circ}\text{C}$ ).

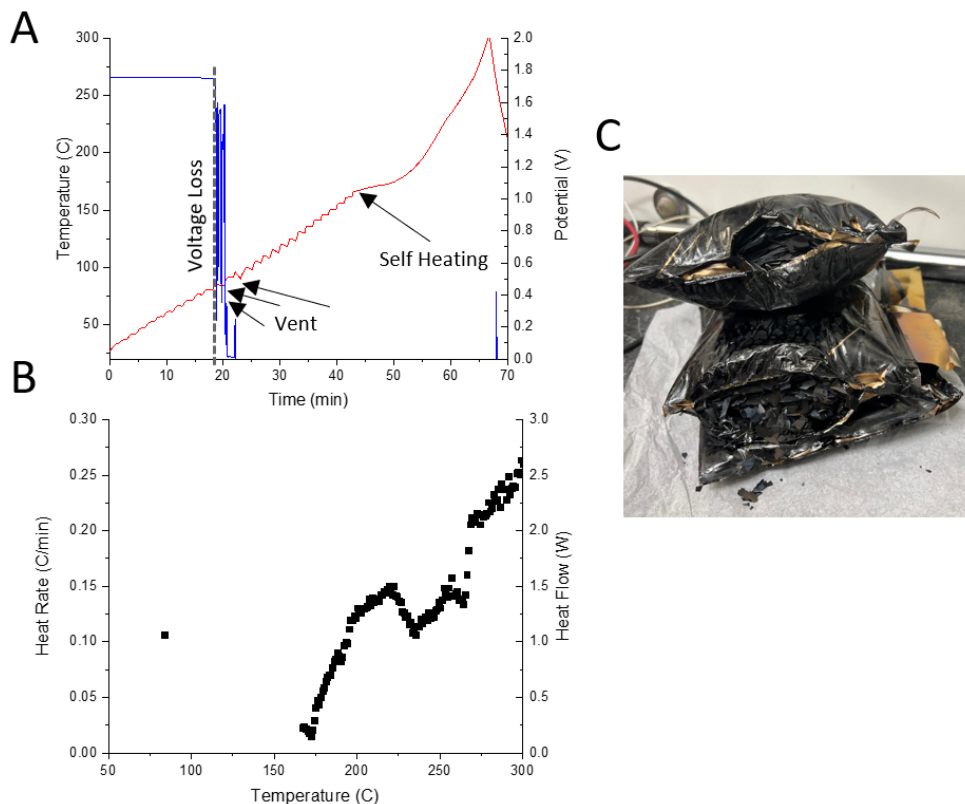


**Figure 7-** **A.** HWS experiments of three 100% SOC Company B cells in a triangle configuration in the ARC ES. Onset of cell self-heating and cell venting on the probed cell. **B** Heat rate and heat flow on the probed cell **C** photograph of the 3 cells after test.

### c. Comparison with LIB

To provide context to the ARC measurements performed on the SIBs, Table 2 includes relevant metrics from ARC tests on NMC and LFP LIBs cells, as well as the Company A and Company B SIBs. Among these metrics the onset temperature, maximum temperature rise, and maximum heat flux are most indicative of transportation risks. The Company A cell exhibits the lowest temperature of self-heating ( $55^{\circ}\text{C}$  or  $131\text{ }^{\circ}\text{F}$ ), which can be achieved during transportation. However, this cell also exhibits the lowest maximum temperature rise.  $0.1^{\circ}\text{C}/\text{min}$ . A rule of thumb for ARC testing is that beyond  $5^{\circ}\text{C}/\text{min}$  thermal runaway and catastrophic failure cannot be prevented. Both LIB types surpass this threshold but neither SIB do. In fact, both SIBs remain below  $0.5\text{ }^{\circ}\text{C}/\text{min}$ .

**Table 2-** Measured values from ARC HWS for SIB and LIB

Cell Type	LIB (NMC)	LIB (LFP)	SIB (Company A)	SIB (Company B)
-----------	-----------	-----------	-----------------	-----------------

Capacity (Ah)	3	1.1	0.7	4.5
Specific heat, $c_p$ (J/gK)	0.9	0.95	1.05	2.0
Mass (g)	45	39	33	305
<b>Onset temp (°C)</b>	<b>125</b>	<b>140</b>	<b>55</b>	<b>170</b>
<b>Max T rise (°C/min)</b>	<b>5000</b>	<b>100</b>	<b>0.1</b>	<b>0.18</b>
Temp at Max Rise (°C)	400	260	120	300
<b>Max Heat flux (W)</b>	<b>3375</b>	<b>62</b>	<b>0.12</b>	<b>2.0</b>
Enthalpy (kJ)	20	7	7.8	78
Heat of reaction (J/g)	600	200	235	256
Data Source	<i>Batteries 2017</i> , 3(2), 14	<i>Batteries 2017</i> , 3(2), 14	this work	this work

ARC measurements allow for enthalpy and heat of reaction from the chemical burning of the cell components. These values prove comparable to that of an LFP LIB, ~200J/g. If we assume a Company B cell burns and dumps all its thermal energy into 2 neighboring cells. The cell's temperature would only rise 64 °C, preventing self-heating of these cells (>150 °C). Alternatively, if a Company A cell fully burned, it would need to dump its thermal energy in to 4 cells to maintain less than 56 °C temperature change. This will not prevent self-heating (>55 °C) but will prevent venting (>100 °C)

$$\Delta T = \frac{Q_{reaction}}{number\ of\ cells \times m \times c_p} \quad (1)$$

The temperature rise was calculated with equation (1), enthalpy of reaction, cell mass, and cell specific heat as reported in Table 1. Cell specific heat was calculated via isothermal mode on the ARC EV for the Company B cell and with isothermal calorimetry (IBC-C) for the Company A cell.

The examined SIBs do not show evidence of catastrophic thermal runaway at 100% SOC and maintain low to mild temperature rise and heat flux when subjected to abusive ARC heat-wait-see tests.

#### IV. Electrochemical Performance

### a. Company A

Company A cells deliver ~0.65 Ah of capacity at a C/2 rate. This value is slightly lower than their 0.7 Ah rating (Figure 8A). The capacity delivered diminishes with charge rate. However high C-rates like 15C or 4 min charge are supported (Figure 8B). Over 100 cycles capacity retention and coulombic efficiency remain stable (Figure 8C).

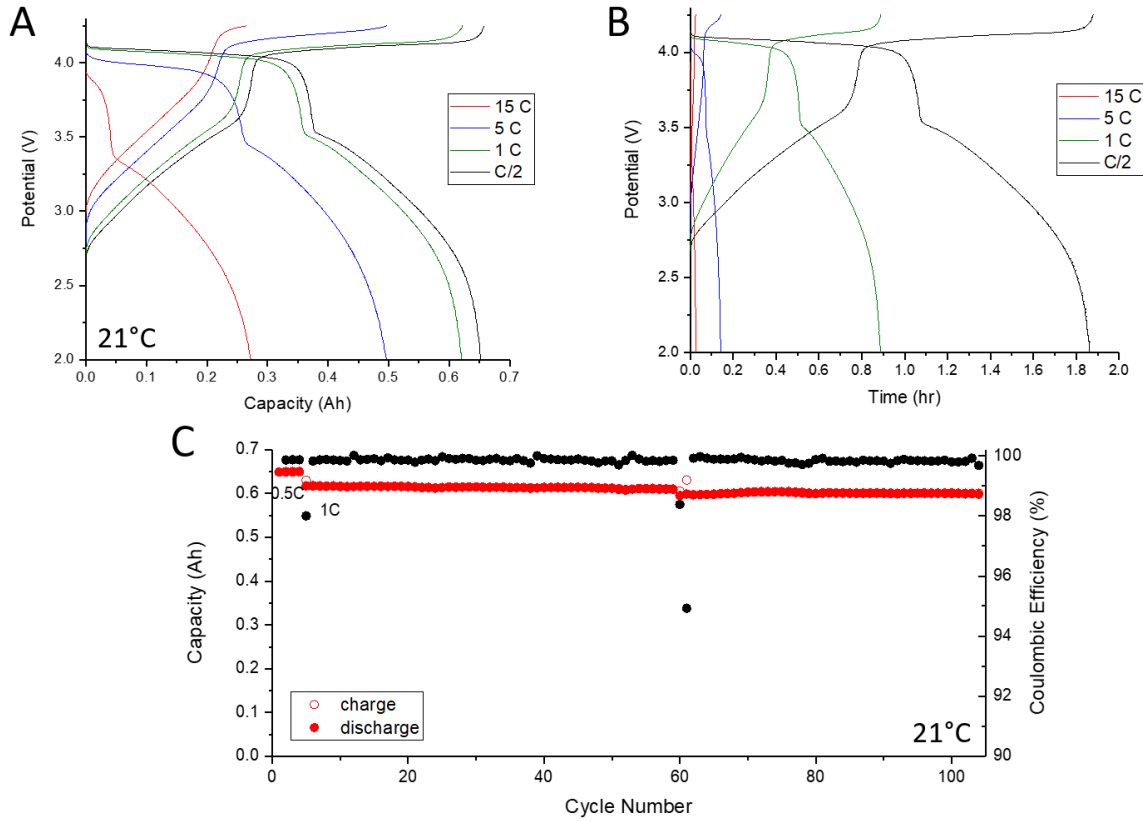


**Figure 8-** Voltage profiles at various C-rate (15, 5, 1, and C/2) with respect to discharge capacity (A) and time (B). C Long-term cycling at 1C.

A notable quality of SIBs is the elimination of the copper current collector, which allows for safe 0V or 0% SOC storage. We examined the 0V storage capability of the Company A cells by completing 4 cycles in the conventional voltage range (2- 4.2V) followed by a 5<sup>th</sup> cycle with discharge to 0V and a 5-hour rest (Figure 9A). After 6 repetitions of this test, substantial capacity loss was observed (Figure 9B), revealing degradation to the cells because of 0V excursions. However, after charging this cell and completing an ARC test at 100% SOC similar failure mode was observed to a pristine 100% SOC cell (Figure 4B), indicating the capacity loss in a Company A cell does not compromise safety.

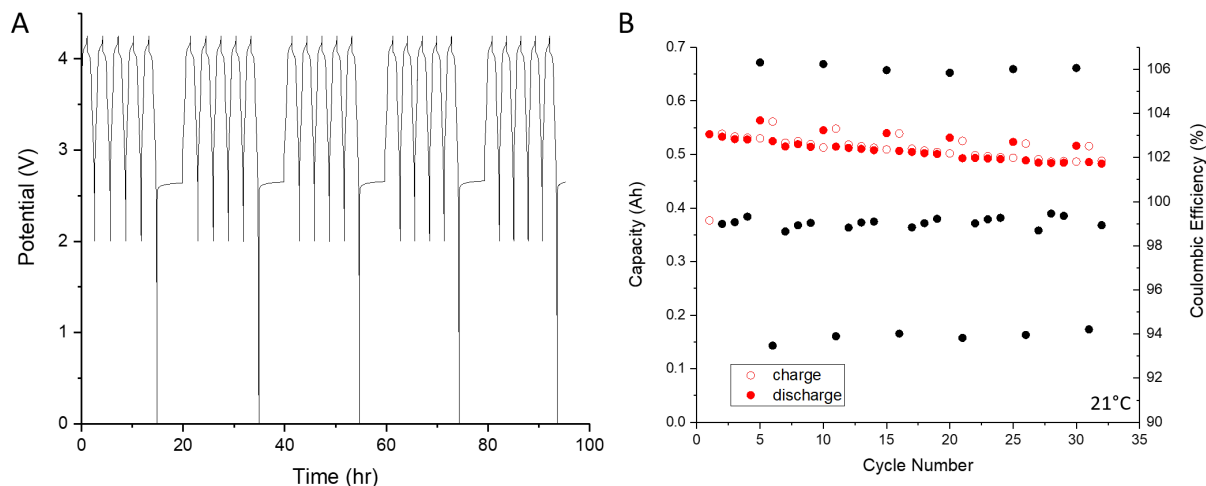


**Figure 9- A** Voltage profiles of 5 galvanostatic 1C cycles followed by an excursion to 0V. This process was repeated for 50 total cycles. Charge and discharge capacity over those 50 cycles are provided in B with open and closed red circles and coulombic efficiency on the right y-axis with black circles.

## b. Company B

Electrochemical analysis like that applied to the Company A cells was completed on the Company B cells. The Company B cells delivered ~4.6 Ah at 1C (Figure 10A), surpassing their rating of 4.3 Ah. We demonstrated cycling up at C-rates up to 4 C or 15-minute charges (Figure 10B). These cells show excellent capacity retention at these high rates. Over 100 cycles the cells exhibit minimal capacity loss or changes to coulombic efficiency (Figure 10C).

Since these cells contain water in their electrolyte, their operation at 0°C or below freezing was of interest. Minimal changes in capacity delivered and capacity loss over 100 cycles was observed (Figure 10D). Additionally, the 0V capability of the Company B cells was examined (Figure 11A). In contrast to the Company A cells, the Company B cells exhibited minimal capacity loss because of the voltage excursion after 6 repetitions. Therefore, 20 repetitions were completed, and still minimal capacity loss was observed. The Company B cell is robust to 0V or 0% SOC storage.

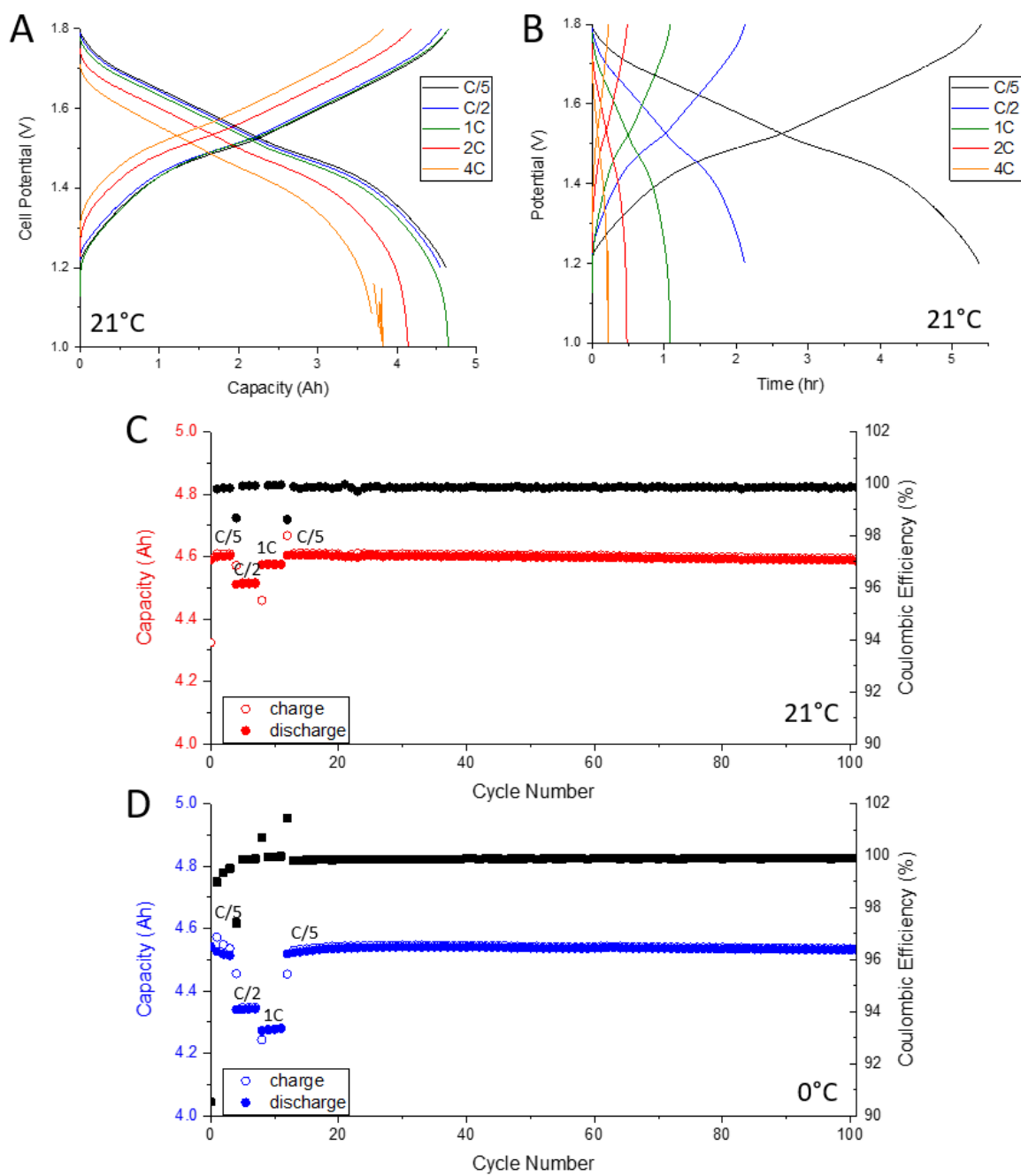


**Figure 10-** Voltage profiles at various C-rate (15, 5, 1, and C/2) with respect to discharge capacity (A) and time (B). Long-term cycling at C/5 at 21°C and 0°C, C and D respectively.

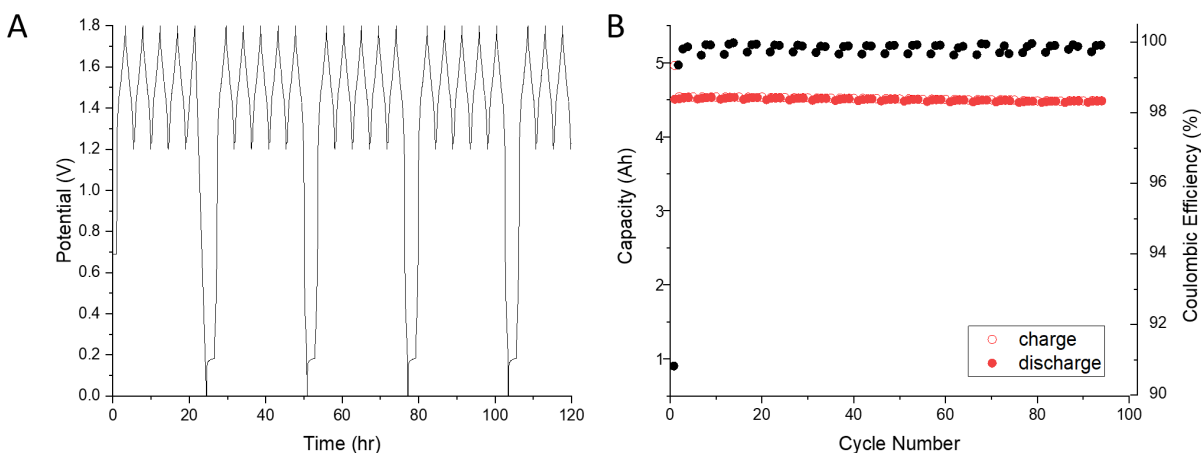


**Figure 11-** A Voltage profiles of 5 galvanostatic C/2 cycles followed by an excursion to 0V. This process was repeated for 100 total cycles. Charge and discharge capacity over those 100 cycles are provided in B with open and closed red circles and coulombic efficiency on the right y-axis with black circles.

### c. Summary

The Company A and Company B cells both exhibit high-rate capability, but the Company B cell proves truer to spec sheet values, and tolerant of 0V or 0% SOC storage.

**Table 3-** Electrochemical specifications and experimentally confirmed values for Company A and Company B

Property	Company A Spec	Company A Test	Company B Spec	Company B Test
Capacity (Ah)	0.7	0.65	4.3	4.6
Nominal Voltage (V)	3.6 (NVP)	3.6	1.8 (aqueous)	1.8
Energy Density (Wh/kg)	80	77	22	23.3
Highest Rate (C, A) Ch	14C, 10A (Ch)	Tested up to 15C at ambient	18C, 80A (Ch)	Tested up to 4C
Discharge	20C, 14A (Dis)		46.5C, 200A (Dis)	
Operating Range (°C)	-30 – 55 °C	Not yet tested	-20 – 45 °C	0°C cycling
0V capable	Yes	Yes	N/A	Yes

## V. Conclusions

Herein we examined Company A and Company B SIB failure modes with HWS ARC measurements. Neither cell exhibited thermal runaway or catastrophic failure modes. Both cells deliver low ( $<5\text{W}$ ) heat release upon material combustion. The Company B cell delivered the most benign failure, likely since it has a water-based electrolyte and low energy density ( $22\text{ Wh/kg}$ ). The Company B cell is a large pouch cell, allowing seal breaching from electrolyte vaporization at  $\sim 100^\circ\text{C}$  and does not exhibit self-heating until temperatures  $>150^\circ\text{C}$ . The peak heat rate during component combustion was  $0.18^\circ\text{C/min}$  or  $2\text{ W}$  of heat flux. The Company A cell has a higher energy density ( $77\text{ Wh/kg}$ ) and contains flammable electrolyte (non-aqueous). This cell exhibits self-heating at milder temperatures,  $55^\circ\text{C}$  or  $131^\circ\text{F}$ . The cell vents its electrolyte at  $\sim 100^\circ\text{C}$  and delivers a peak heat rate of  $0.1^\circ\text{C/min}$  or  $0.12\text{ W}$ .

Using isothermal mode in the ARC EV and isothermal calorimetry we assessed the specific heat of the Company A and Company B cell, respectively. The specific heat of the Company B cell is  $1.05\text{ J/(g}^\circ\text{C)}$  and the Company A is  $2.0\text{ J/(g}^\circ\text{C)}$ . A conventional LIB has specific heat of  $\sim 0.9\text{ J/(g}^\circ\text{C)}$ . SIBs have higher specific heat because of the use of aluminum at both current collectors and the Company B cell is higher than the Company A due to the water-based electrolyte (specific heat of water  $4.2\text{ J/(g}^\circ\text{C)}$ ). With this information, we can calculate how much adjacent cells will heat if a single cell combusts. If a Company B cell combusts and rejects all its thermal energy into 2 neighboring cells, the neighboring cells will increase in temperature by  $64^\circ\text{C}$ . Even in a warm ambient condition ( $40^\circ\text{C}$  or  $104^\circ\text{F}$ ), this will not be enough heating to cause self-heating of the neighboring cells, which is observed at  $\sim 150^\circ\text{C}$ . Alternatively, the Company A cell exhibits self-heating at a milder temperature  $55^\circ\text{C}$ , which will be difficult to avoid if a cell is combusting. However, if a Company A cell is combusting and rejects its thermal energy into 4 neighbors, the neighbors will experience a temperature rise of  $56^\circ\text{C}$ , allowing self-heating but maintaining the cells below their vent temperature ( $100^\circ\text{C}$ ). Packaging components can have specific heats as high as  $1000\text{ J/(g}^\circ\text{C)}$  which will consume the heat of a failing SIB with minimal ( $<10^\circ\text{C}$ ) temperature change.

An advantage of SIBs over LIBs is the ability to store SIBs at  $0\text{V}$  or  $0\%$  SOC. We examined the influence of  $0\text{V}$  storage on safety and performance for both the Company A and Company B cells. Company B cells remained robust to  $0\text{V}$  storage and cycling. No degradation was observed. Company A cells exhibited capacity fade after  $0\text{V}$  storage, indicating degradation to the cell. However, when subjected to ARC testing the Company A cells degraded by  $0\text{V}$  storage delivered similar failure modes to pristine Company A cells.

In future work we will analyze the vent gas of the Company A and Company B cells to determine toxicity and flammability. This is a hazard not addressed by ARC measurements. Additionally impact testing of the cells will be performed. Follow on efforts will explore the influence of high total energy SIBs ( $>10\text{ Ah}$ ) and high energy density SIBs ( $>100\text{ Wh/kg}$ ). Higher energy or higher energy density can result in more catastrophic failure modes and perhaps thermal runaway.

## References

- (1) Peters, J. F.; Peña Cruz, A.; Weil, M. Exploring the Economic Potential of Sodium-Ion Batteries. *Batteries* **2019**, 5 (1), 10.
- (2) Tapia-Ruiz, N.; Armstrong, A. R.; Alptekin, H.; Amores, M. A.; Au, H.; Barker, J.; Boston, R.; Brant, W. R.; Brittain, J. M.; Chen, Y.; et al. 2021 roadmap for sodium-ion batteries. *Journal of Physics: Energy* **2021**, 3 (3), 031503. DOI: 10.1088/2515-7655/ac01ef.
- (3) Lei, B.; Zhao, W.; Ziebert, C.; Uhlmann, N.; Rohde, M.; Seifert, H. J. Experimental Analysis of Thermal Runaway in 18650 Cylindrical Li-Ion Cells Using an Accelerating Rate Calorimeter. In *Batteries*, 2017; Vol. 3.
- (4) Carter, R.; Klein, E. J.; Kingston, T. A.; Love, C. T. Detection of Lithium Plating During Thermally Transient Charging of Li-Ion Batteries. *Frontiers in Energy Research* **2019**, 7, Original Research. DOI: 10.3389/fenrg.2019.00144.